



# Cellulose cryogel particles for oil structuring: Mixture properties and digestibility

Francesco Ciuffarin<sup>a</sup>, Stella Plazzotta<sup>a</sup>, Loris Gelas<sup>b</sup>, Sonia Calligaris<sup>a,\*</sup>, Tatiana Budtova<sup>b</sup>, Lara Manzocco<sup>a</sup>

<sup>a</sup> Department of Agricultural, Food, Environmental and Animal Sciences, University of Udine, Via Sondrio 2/A, 33100, Udine, Italy

<sup>b</sup> MINES Paris, PSL University, Center for Materials Forming (CEMEF), UMR CNRS 7635, CS 1027, Rue Claude Daunesse, 06904, Sophia Antipolis, France

## ARTICLE INFO

### Keywords:

Freeze-drying  
Cellulose  
Porosity  
Oleogel  
Rheological properties  
Digestion

## ABSTRACT

This study evaluated the feasibility of using cellulose cryogel particles to structure liquid oil. To this aim, cryogel particles were prepared by grinding and freeze-drying a hydrogel made from a 5% (w/w) microcrystalline cellulose (MCC) dissolved in aqueous NaOH and coagulated in water. Compared to native MCC, cryogel particles presented a more irregular surface, as detected by scanning electron microscopy. The powder of cryogel particles presented low density ( $0.25 \text{ g cm}^{-3}$ ), and high porosity (78%). The obtained particles were mixed with increasing quantities of sunflower oil, from 60 to 80% (w/w) oil, and their capacity to entrap oil forming a semi-solid material was determined. While MCC showed no oil structuring capacity, cellulose cryogel particles mixed with 71–74% (w/w) oil resulted in gel-like materials characterized by 100% oil holding capacity. No oil was released upon temperature increase up to  $90 \text{ }^\circ\text{C}$ . The compressive behavior of these systems revealed no yield point, highlighting a non-spreadable deformation behavior. In these conditions, cellulose cryogel particles likely absorbed oil in their pores, while free oil formed capillary bridges allowing particle interconnections without the formation of a plastic network. Based on these considerations, these materials can be regarded as granular solids. The *in vitro* gastrointestinal digestion showed that oil structuring by cellulose cryogel particles did not affect the kinetics or the extent of fatty acid release. The proposed oil structuring approach opens promising applications of porous cellulose in foods.

## 1. Introduction

Today, it is recognized that the excessive consumption of saturated (SFA) and *trans* fatty acids (TFA) is associated with the onset of different diet-related diseases, such as obesity and cardiovascular diseases (Silva, Ferdous, Foguel, & da Silva, 2023). Traditional food fats, such as palm oil, coconut oil, hydrogenated oils, and animal fats, are particularly rich in SFA (Hooper et al., 2020). SFA form crystalline networks responsible for the unique fat semi-solid and spreadable structure, which imparts distinctive technological and sensory characteristics to SFA-rich food products, highly appreciated by consumers. Based on these considerations, the substitution of traditional fats with liquid oils, rich in healthy unsaturated fatty acids, is considered a priority to favor healthful dietary patterns (Hooper et al., 2020). However, the substitution should ensure the retention of the technological and sensory properties of traditional fats, to secure consumer acceptance (Martins, Vicente, Cunha, & Cerqueira, 2018).

In this context, the field of oleogelation is rapidly evolving. Oleogelation refers to strategies aiming at converting liquid oils into gel-like materials, namely oleogels, able to efficiently mimic the technological properties of SFA-rich fats (Marangoni & Garti, 2018; Martins et al., 2018; Zhao, Wei, & Xue, 2022). Besides their role as fat alternatives, oleogels have also been studied for their potential to steer lipid digestibility (Ashkar, Laufer, Rosen-Kligvasser, Lesmes, & Davidovich-Pinhas, 2019; Calligaris, Alongi, Lucci, & Anese, 2020; Ciuffarin, Négrier, et al., 2023; Marangoni et al., 2007; O'Sullivan, Davidovich-Pinhas, Wright, Barbut, & Marangoni, 2017; Plazzotta et al., 2022) and bioaccessibility of lipophilic compounds (Calligaris et al., 2020; Dent, Hallinan, Chitchumroonchokchai, & Maleky, 2022; Luo, Ye, Wolber, & Singh, 2021; Salvia-Trujillo et al., 2017; Zhao et al., 2022).

Currently, two main strategies have been proposed in the literature for oleogelation. Direct oleogelation refers to the solubilization of liposoluble structuring agents in oil at high temperatures, followed by controlled cooling, which leads to the formation of a self-assembled

\* Corresponding author.

E-mail address: [sonia.calligaris@uniud.it](mailto:sonia.calligaris@uniud.it) (S. Calligaris).

<https://doi.org/10.1016/j.foodhyd.2024.110470>

Received 27 February 2024; Received in revised form 23 July 2024; Accepted 25 July 2024

Available online 27 July 2024

0268-005X/© 2024 The Authors. Published by Elsevier Ltd. This is an open access article under the CC BY license (<http://creativecommons.org/licenses/by/4.0/>).

network. Conversely, indirect oleogelation exploits hydrophilic biopolymers (e.g., proteins and carbohydrates), properly structured to interact with oil (Martins et al., 2018; Patel, 2020; Schatteman, 2013). Both strategies have advantages and disadvantages, associated with the type and concentration of the applied molecules as well as the processing costs and sustainability (Sabet, Pinto, Kirjoranta, Garcia, & Valoppi, 2023). Direct methods are simple to perform but rely on the use of gelators, most of which are classified as additives, hardly fitting in the current “clean-label” context. On the opposite, indirect methods are based on the use of hydrocolloids, such as polysaccharides and proteins, which usually do not fall under the classification of additives, and whose consumption is often associated with health benefits. However, indirect approaches require multi-step procedures to overcome the intrinsic incompatibility of hydrophilic structuring agents with oil (Manzocco, Mikkonen, & García-González, 2021). Among indirect methods, the dried-template approach is based on the initial formation of an aqueous gel or hydrogel. Water is subsequently removed from the hydrogel by using different techniques (i.e., freeze- or supercritical-CO<sub>2</sub>-drying), resulting in highly porous dry templates, showing the ability to load and entrap liquid oil.

In this regard, one promising biopolymer for indirect oleogelation via the dried template approach is cellulose, which is naturally present in many foods and widely used at the industrial level for its functional properties and benefits. According to a recent European Food Safety Authority (EFSA) re-evaluation, the use of cellulose derivatives is not associated with adverse health effects, so there is no need for a numerically acceptable daily intake (Younes et al., 2018). For this reason, cellulose and its derivatives are commonly added to various food products, serving as thickeners, stabilizers, fillers, and bulking agents in products such as sauces, dressings, and dairy alternatives (Mu et al., 2019). Consumers are familiar with cellulose as an ingredient, and its popularity is growing due to its plant origin and associated health benefits. Being non-digestible, cellulose contributes to reducing food caloric intake and promotes gastrointestinal health, acting as a prebiotic for gut microbes (Hervik & Svihus, 2019; Uddin, Mahmud, Hasan, Peltoniemi, & Oliviero, 2023). Additionally, cellulose can be retrieved from agro-industrial vegetable side streams, supporting sustainable practices of circular economy (Plakantonaki, Roussis, Bilalis, & Priniotakis, 2023).

Cellulose and its derivatives have been scarcely considered for oleogelation by indirect methods. Carboxymethylcellulose was proposed as a structuring agent in combination with other biopolymers to form structured emulsions, which have been converted into oleogels through drying (i.e., emulsion template approach) (Jiang et al., 2018; Meng, Qi, Guo, Wang, & Liu, 2018). In our recent work, we demonstrated the ability of macro-porous cryogel monoliths, obtained by freeze-drying hydrogels made of dissolved and coagulated microcrystalline cellulose (MCC), to load high quantities of sunflower oil, begetting solid materials with high physical stability and no oil release during storage (Ciuffarin, Négrier, et al., 2023). However, these monoliths showed physical properties far from the ones required for their use as fat alternatives. To solve this issue, a possible strategy could involve oil structuring by cellulose porous particles instead of monoliths. Dried porous particles made of proteins derived from whey (De Vries, Gomez, Van der Linden, & Scholten, 2017; Plazzotta, Calligaris, & Manzocco, 2020), potato (Jung et al., 2023), and egg white (Alavi & Ciftci, 2023) have been reported to form semi-solid oleogels. This was attributed to concomitant mechanisms concurring in oil structuration by the dried protein particles, namely (i) absorption of oil into particle pores; (ii) adsorption of the oil onto the particle surface; (iii) formation of oil capillary bridges among the particles and (iv) physical entrapment of free oil within a hydrophilic particle-particle network (Selmer et al., 2019).

Based on these considerations, the objective of this work was to explore the oil structuring ability of cellulose cryogel particles. To this aim, MCC was dissolved in aqueous NaOH, gelled and coagulated in

water forming a hydrogel. The latter was ground and freeze-dried. The obtained cellulose cryogel particles were sieved to collect the <100 µm fraction, which was characterized for its porosity, density, BET-specific surface area and SEM microstructure. Cellulose cryogel particles were dispersed in sunflower oil at different particle-to-oil ratios. The obtained materials were then studied for their rheological properties, spreadability, and oil-holding capacity to investigate whether this oleogelation approach resulted in fat-mimicking physical properties. Finally, the impact of cellulose oleogelation on lipid digestibility was evaluated with *in vitro* digestion tests.

## 2. Materials and methods

### 2.1. Materials

Microcrystalline cellulose (MCC, Avicel®, pH-101, degree of polymerization 180 as declared by the manufacturer) and NaOH were purchased from Sigma Aldrich (Milan, Italy). Sunflower oil was obtained from a local store. Deionized water was made with System Advantage A10® (Millipore S.A.S, Molsheim, France).

### 2.2. Cryogel particles

Cellulose hydrogel monoliths were prepared according to Ciuffarin, Négrier, et al. (2023) from MCC. Briefly, MCC was dissolved in aqueous NaOH solution (8%, w/w) at −5 °C for 2 h, resulting in a MCC solution at 5% (w/w). The solution was gelled at 50 °C for 2 h, and coagulated in deionized water, followed by several washing steps with water.

Hydrogel monoliths were placed in deionized water (2:1, w/w) and ground using a high-speed homogenizer (DI 25 Basic, IKA Werke, Staufen im Breisgau, Germany) at 14,000 rpm for 3 min. The obtained dispersion was placed in aluminium trays (8 × 15 cm), frozen at −40 °C for 45 min in a blast chiller (FAB25 Electrolux, Italy), and finally freeze-dried. The freeze-dryer (EPSILON 2–4 LSCplus, Del Tek, Naples, Italy) was set at 0.2 mBar and the following steps were performed: 20 min at −30 °C, 24 h at −20 °C, 24 h at −10 °C, 8 h at 0 °C, 16 h at 10 °C, and finally at 20 °C for 8 h. The resulting cellulose cryogel particles were stored at room temperature in a desiccator containing silica until use.

The cryogel particles were finally sieved (FTS-0200, Filtra Vibracion, Barcelona, Spain) and the fraction with size <100 µm was used to prepare oleogels.

### 2.3. Mixtures of cryogel particles and oil

About 1.0 g of cryogel particles was manually mixed with different amounts of sunflower oil (SO), leading to systems with an oil content ranging from 65 to 80% (w/w).

### 2.4. Characterization of cryogel particles

#### 2.4.1. Image acquisition

Sample images were acquired using an image acquisition cabinet and a Google Pixel 6 smartphone (Alphabet, Mountain View, California, USA). The light was provided by a LED strip properly placed to minimize shadow and glare.

#### 2.4.2. Particle size distribution

An amount of 5 g of cryogel particles was sieved with a set of sieves with mesh sizes of 25 and 50 µm (FTS-0200, Filtra Vibracion, Barcelona, Spain). The amount of powder remaining in each sieve was weighed and expressed as a percentage of the initial powder weight.

#### 2.4.3. Tap density

The cryogel particles or MCC particles (0.5 g) were placed into a graded cylinder (1.5 cm in diameter) and weighed, after manual tapping. The tap density of the powder was then calculated from the

powder mass ( $m$ ) and tap volume ( $V_t$ ) (Eq. (1)):

$$\rho_t = \frac{m}{V_t} \quad (\text{Eq. 1})$$

#### 2.4.4. Porosity

Cryogel powder porosity (%) was estimated based on the following equation (Eq. (2)) (Druel, Niemeyer, Milow, & Budtova, 2018):

$$\text{Porosity (\%)} = \left(1 - \frac{\rho_t}{\rho}\right) \bullet 100 \quad (\text{Eq. 2})$$

where  $\rho_t$  ( $\text{g cm}^{-3}$ ) is the tap density of the powder and  $\rho$  ( $\text{g cm}^{-3}$ ) is cellulose true density (i.e., skeletal density). In particular,  $\rho$  was considered as MCC true density ( $\rho = 1.46 \text{ g cm}^{-3}$ ) (Sun, 2005).

#### 2.4.5. Morphology

SEM micrographs were obtained using an MAIA-3 (Tescan, Brno, Czech Republic), equipped with detectors of secondary and back-scattered electrons. Cryogel particles were deposited on carbon tape and their surface was coated with a 14 nm layer of platinum with a Quorum Q150T metallizer (Quorum Technologies, East Sussex, UK) to prevent the accumulation of electrostatic charges and image defaults. The observations were performed with an acceleration voltage of 3 kV and the images acquired with an accumulation of three frames.

#### 2.4.6. Specific surface area

The specific surface area ( $S_{\text{BET}}$ ) was determined by measuring  $\text{N}_2$ -adsorption isotherm at 77 K with the Micromeritics ASAP 2020 (Norcross, Georgia, USA) and using the Brunauer–Emmett–Teller (BET) approach (Brunauer, Emmett, & Teller, 1938). Before measurements, samples were degassed under high vacuum for 10 h at 70 °C.

### 2.5. Characterization of mixtures of cryogel particles and oil

#### 2.5.1. Rheological properties

The viscoelastic properties (moduli  $G'$ ,  $G''$  and  $\tan \delta$ ) of the cryogel-oil mixtures were tested using an RS6000 Rheometer (Thermo Scientific RheoStress, Haake, Germany), equipped with a Peltier system for temperature control. Measurements were performed using a parallel plate geometry at 20 °C with a gap of 2.0 mm. Oscillatory sweep tests to identify the linear viscoelastic region (LVR) were performed increasing stress from 10 to  $1 \times 10^4$  Pa at 1 Hz frequency. Yield stress (Pa) was identified as the stress value corresponding to a 10% drop in  $G'$  value. Frequency sweep tests were then performed increasing frequency from 0.1 to 10 Hz at stress values selected in the LVR (100 Pa). Temperature sweep tests were carried out at 1 Hz and a stress value within the LVR, by increasing the temperature from 20 to 90 °C, with a heating rate of 1 °C  $\text{min}^{-1}$ .

#### 2.5.2. Spreadability

Spreadability was measured by a uniaxial compression test using an Instron 4301 (Instron LTD., High Wycombe, UK). In brief, 2 mL of oleogel was transferred in a 5 mL glass beaker with a diameter of 1.5 cm and compressed 5 mm using an 8.1 mm diameter cylindrical probe mounted on a 500 N compression head at a 25  $\text{mm min}^{-1}$  crosshead speed. Stress-strain curves were obtained from the compression tests and fitted using Microsoft Office Excel (LTSC Professional Plus 2021).

#### 2.5.3. Oil holding capacity

About 1 g of cryogel-oil mixture was placed into a microcentrifuge tube and centrifuged at  $14,900 \times g$  for 20 min at 20 °C (Mikro 120, Hettich Zentrifugen, Andreas Hettich GmbH and Co, Tuttlingen, Germany). The separated oil phase was accurately drained with absorbent paper and the sediment weighed. The oil holding capacity (OHC) was expressed as the percentage of oil retained by the sample as compared to the initial oil content.

### 2.6. In vitro lipid digestibility

#### 2.6.1. In vitro digestion

The *in vitro* digestion process followed the INFOGEST static protocol (Brodkorb et al., 2019), and the pH-stat approach was used to determine the extent of lipid digestibility (Mat, Le Feunteun, Michon, & Souchon, 2016), by replacing NaCl with  $\text{NaHCO}_3$  in simulated salivary (SSF), gastric (SGF), and intestinal (SIF) fluids. The formulation containing 71% oil (i.e., 1.4 g of cellulose-based oleogel, corresponding to 1  $\text{g}_{\text{oil}}$ ) was used.

SSF, SGF, and SIF were preheated to 37 °C. As the to-be-digested samples were free from starch and proteins, amylolytic and proteolytic enzymes were not used.

For the oral phase, 4 mL of SSF, 25  $\mu\text{L}$  of 0.3 M  $\text{CaCl}_2$ , and 975  $\mu\text{L}$  of water were added to the samples, which were continuously stirred at 37 °C for 2 min.

In the gastric phase, 8 mL of SGF, 5  $\mu\text{L}$  of 0.3 M  $\text{CaCl}_2$ , and 667  $\mu\text{L}$  of water were added to the oleogel sample. The gastric phase was initiated by adjusting the pH to 3.0 with 1 M HCl and making up the volume to 20 mL with water. The mixture was continuously stirred at 37 °C for 2 h.

In the intestinal phase, 8 mL of SIF, 4  $\mu\text{L}$  of 0.3 M  $\text{CaCl}_2$ , 5 mL of a lipase solution (prepared in SIF and providing 2000  $\text{U mL}^{-1}$  activity), and 3 mL of 160 mM bile extract (prepared in SIF) were added to cellulose oleogel. The intestinal phase was initiated by adjusting the pH to  $8.00 \pm 0.10$  with 1 M NaOH and making up the volume to 40 mL with water. The pH of the digestion mixture was monitored immediately after lipase addition and 0.25 M NaOH aliquots were automatically added by a TitroLine® 7000 titrator (SI Analytics GmbH, Mainz, Germany) to maintain a value of  $8.0 \pm 0.025$  (i.e., the optimum of used lipase based on its technical specifications). The volume of NaOH (mL) added to titrate the oleogels at a specific time was recorded ( $V_{\text{oleogel}}$ ).

The percentage of free fatty acids (FFA) released during lipolysis was calculated (Eq (1)):

$$\text{FFA (\%)} = \frac{V_e}{V_t} \times 100 \quad \text{Eq. 1}$$

where  $V_e$  is the experimental volume of the oil, and  $V_t$  represents the theoretical volume required to titrate the fatty acids released by complete hydrolysis of triglycerides in the reaction vessel, assuming that 2 FFA are produced for each triacylglycerol molecule (Li, Hu, Du, Xiao, & McClements, 2011), and was calculated according to Eq. (2):

$$V_t = 2 \times \left[ \frac{m_{\text{oil}}}{MW_{\text{oil}}} \frac{1000}{C_{\text{NaOH}}} \right] \quad \text{Eq. 2}$$

where  $m_{\text{oil}}$  is the mass of oil in the reaction vessel (g),  $MW_{\text{oil}}$  is the average molecular weight of sunflower oil ( $876.60 \text{ g mol}^{-1}$ , Plazzotta et al., 2022) and  $C_{\text{NaOH}}$  is the concentration of the sodium hydroxide ( $\text{mol L}^{-1}$ ).

After *in vitro* digestion, the digestion was stopped by placing the sample into an ice bath for 15 min, centrifuged at  $30,000 \times g$  for 70 min using an Avanti J-25 centrifuge (Beckman, Palo Alto, USA), and a 30 mL aliquot of the mixed micellar phase (i.e., stabilized structures encapsulating lipophilic bioactive components) was recovered.

#### 2.6.2. Confocal microscopy of digested samples

The hanging-drop method was used to analyze samples collected after the gastric and intestinal digestion phases (i.e., digestate) (Gallier, Gordon, & Singh, 2012). Samples were stained by gently hand-mixed with 0.05 mL of a 0.2% (w/v) aqueous solution of Nile Red and 0.01% (w/v) of Fluorescent Brightener 28 (Sigma Aldrich, Milan, Italy), to selectively mark the oil and the cellulose fraction, respectively. Secondly, an agarose solution (1%, w/w) preheated at 50 °C, was added to the samples in a sample:agarose solution ratio of 1:2 (v/v). Two  $\mu\text{L}$  of the fluid mix was placed on a microscope coverslip and left to set at room temperature for 1 min. The stained samples were then placed on a

microscope slide, covered with a cover slide, and observed using a confocal laser scanning microscope at 100 × magnification (Leica TCS SP8 × confocal system, Leica Microsystems, Wetzlar, Germany). Images were imported in jpg format using the software LasX 3.5.5 (Leica Microsystems, Wetzlar, Germany).

### 2.6.3. Particle size and zeta potential of mixed micellar phase

The particle size distribution of the mixed micellar phase (recovered as described in section 2.6.1) was determined using Dynamic Light Scattering (DLS) with a Zetasizer NanoZS (Malvern Instruments, Worcestershire, UK). Samples were diluted 1:100 (v/v) with deionized water and introduced into a measuring cell where the particles scattered laser light at a 173° angle. Particle size was expressed by the average diameter, considering the total volume of particles. Additionally, the  $\zeta$ -potential was measured by placing the diluted sample in a capillary cell equipped with two electrodes to assess particle electrophoretic mobility.

### 2.7. Data analysis

Data were expressed as the mean ± standard error of at least two measurements from two experimental replicates ( $n \geq 3$ ). Statistical analysis was performed by using R v. 4.0.3 (The R Foundation for Statistical Computing). The ANOVA test was used to determine statistically significant differences between means ( $p < 0.05$ ). Bartlett's test was used to check the homogeneity of variance ( $p \geq 0.05$ ) and the Tukey test was used as a posthoc test ( $p < 0.05$ ).

## 3. Results and discussion


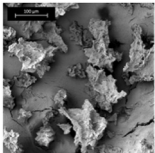
### 3.1. Cellulose cryogel particles

Table 1 shows macroscopic and microscopic features, particle size distribution, tap density, porosity, and  $S_{BET}$  of the powder based on cellulose cryogel particles obtained by grinding cellulose hydrogels made from 5% (w/w) cellulose solutions.

As shown in Table 1, cellulose cryogel powder contained particles with dimensions mainly in the range of 50–100  $\mu\text{m}$  (60%) and 25–50  $\mu\text{m}$  (40%). The particles showed irregular shapes, sharp edges, and uneven surfaces. Similar morphology has been previously observed for particles obtained by freeze-drying and grinding of whey protein hydrogels as well as for freeze-dried particles containing a combination of maltodextrin with  $\kappa$ -carrageenan or soybean protein (Papoutsis et al., 2018; Plazzotta et al., 2020). The morphology of cellulose cryogel particles was different from that of the initial MCC particles, which are characterized by elongated shape, compact non-porous structure, and smooth surface (Mahdi, Hassanpour, & Muller, 2018). The density and the porosity of the cryogel powder (Table 1) were respectively lower and higher than those of the native MCC powder (tap density 0.42  $\text{g cm}^{-3}$ ; porosity 71%). The internal surface area ( $S_{BET}$ ) of cryogel powder, which is related to the presence of mesopores, was also higher (4.8  $\text{m}^2 \text{g}^{-1}$ ) than that of the MCC (0.59–0.93  $\text{m}^2 \text{g}^{-1}$ , Vehovec, Gartner, Planinček, & Obreza, 2012; Mahdi et al., 2018).

**Table 1**

Characteristics of cellulose cryogel powder: appearance, microstructure (scale is 100  $\mu\text{m}$ ), particle size distribution, tap density, porosity, and specific surface area ( $S_{BET}$ ).

Macroscopic Appearance	SEM microstructure	Particle size distribution (%)			Tap density ( $\text{g cm}^{-3}$ )	Porosity (%)	$S_{BET}$ ( $\text{m}^2 \text{g}^{-1}$ )
		50–100 $\mu\text{m}$	25–50 $\mu\text{m}$	<25 $\mu\text{m}$			
		59.4 ± 0.3	40.3 ± 0.8	0.2 ± 0.1	0.25 ± 0.01	78.4 ± 0.5	4.8 ± 0.9

Overall, the procedure applied to convert cellulose hydrogels into cryogel particles led to the formation of a powder formed by particles with rough surfaces, and characterized by lower tap density and higher porosity compared to the native MCC powder.

### 3.2. Systems containing cellulose cryogel particles and sunflower oil

To assess its capacity to structure oil, the powder of cellulose cryogel particles was manually mixed with sunflower oil at different cellulose cryogel powder/oil ratios, and the obtained systems were characterized. The formation of a semi-solid material resembling an oleogel was visually evaluated by assessing the ability of the mixtures to form a cohesive and continuous material able to stick to the spatula when turned upside-down. As shown in Fig. 1, at oil content lower than 71% (w/w), the cryogel-oil mixtures resulted in a grainy system with visible aggregates of particles unable to stick together. In these samples, the oil was probably mainly absorbed into the inner pores, with no interaction among particles.

By contrast, in an oil range of 71–74% (w/w), materials with a creamy appearance and no evident oil release were obtained. In this case, the oil was probably not only absorbed in the inner pores of cryogel particles but also engaged in the formation of capillary bridges among the walls of adjacent cellulose particles (Selmer et al., 2019). Finally, upon increasing oil content above 74% (w/w), the samples showed a liquid-like behavior. Analogous trends were previously reported by Jung et al. (2023), considering mixtures of whey and potato protein porous powders with oil in the oil content range of 70–84% (w/w). It must be pointed out that, in the same conditions, the MCC powder exhibited no ability to structure oil. MCC mixing with oil led to liquid systems showing evident oil release, regardless of the oil content (Fig. 1).

To better understand the oil structuring capability of cellulose cryogel particles, the creamy systems obtained in the oil content range from 71 to 74% were considered for further analyses.

The influence of oil content on the rheological properties of the systems is presented in Fig. 2 and Table 2. All the samples exhibited a gel-like behavior, with the elastic modulus ( $G'$ ) being higher than the viscous one ( $G''$ ). With the increase in oil content, the yield stress (i.e., the limit of the linear viscoelastic region, LVR) and both the storage ( $G'$ ) and loss ( $G''$ ) moduli decreased (Fig. 2A–Table 2).

The viscoelastic behavior of the samples was further investigated through frequency sweep analysis (Fig. 2B). The moduli  $G'$  and  $G''$  exhibited parallel patterns, unaffected by the applied frequency. Moreover, all systems showed a very low  $G''/G'$  ratio (i.e.,  $\tan \delta$ , Table 2), indicating a solid-like nature. The increase in oil concentration above 71% resulted in a slight increase in  $\tan \delta$  (Table 2). The rheological properties of the cellulose cryogel-containing samples (Fig. 2, Table 2) were comparable to those reported for oleogels obtained through the dried template approach using both whey and potato proteins (Jung et al., 2023; Plazzotta et al., 2021). In the literature,  $G'$  and yield stress are often suggested as key parameters to compare the rheological properties of fat replacers with those of traditional fats (Blake & Marangoni, 2015). For instance, these parameters were used to demonstrate

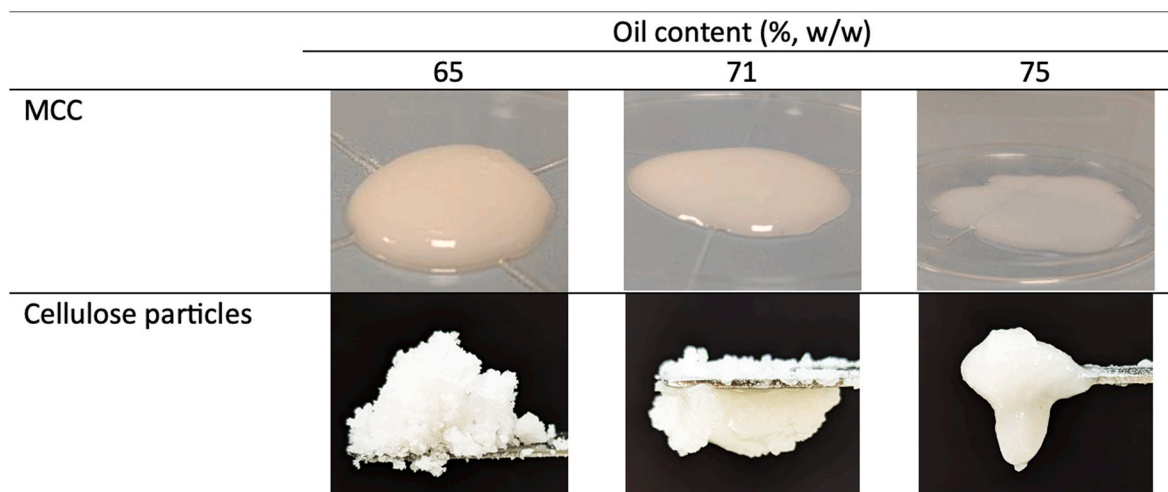


Fig. 1. Visual appearance of systems containing microcrystalline cellulose (MCC) or cellulose cryogel particles and increasing concentrations of sunflower oil.

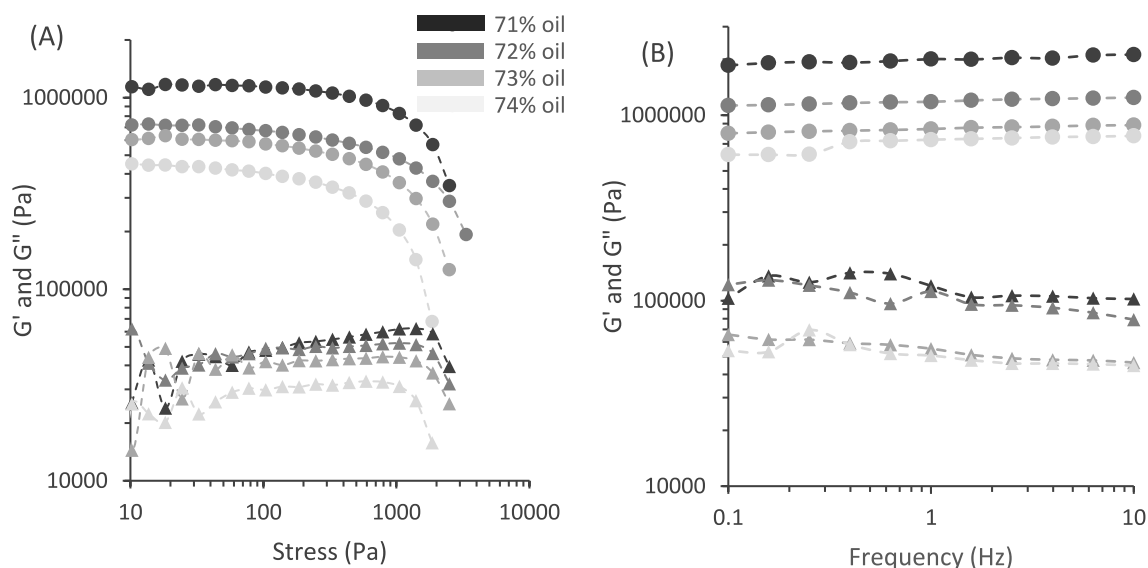


Fig. 2.  $G'$  (circles), and  $G''$  (triangles) from amplitude (A) and frequency sweeps (B) of systems containing cellulose cryogel particles and increasing concentrations of sunflower oil from 71 to 74% (w/w). Standard deviation bars were omitted to improve graph readability.

Table 2

Rheological parameters (yield stress,  $G'$ ,  $G''$  and  $\text{Tan } \delta$  in the linear region) of systems containing cellulose cryogel particles and increasing concentrations of sunflower oil.

Oil (% w/w)	Yield stress (Pa)	$G' \times 10^5$ (Pa)	$G'' \times 10^5$ (Pa)	$\text{Tan } \delta$
71	403.0 ± 62.3 <sup>a</sup>	21.3 ± 1.8 <sup>a</sup>	1.2 ± 0.0 <sup>a</sup>	0.055 ± 0.006 <sub>b</sub>
72	154.4 ± 26.9 <sup>b</sup>	10.6 ± 1.5 <sup>b</sup>	0.7 ± 0.1 <sup>b</sup>	0.072 ± 0.001 <sub>a</sub>
73	142.8 ± 40.9 <sup>b</sup>	8.1 ± 0.4 <sup>c</sup>	0.5 ± 0.0 <sup>c</sup>	0.070 ± 0.002 <sub>a</sub>
74	127.3 ± 20.1 <sup>b</sup>	1.4 ± 0.3 <sup>d</sup>	0.1 ± 0.0 <sup>d</sup>	0.068 ± 0.001 <sub>a</sub>

<sup>a-d</sup>: In the same column, mean values indicated by different letters are statistically different ( $p < 0.05$ ).

the suitability as fat replacers of structured monoglyceride-based emulsions and oleogels structured by means of porous protein particles (Blake & Marangoni, 2015; Calligaris, Plazzotta, Barba, &

Manzocco, 2021; Plazzotta et al., 2020). Notably, the values displayed in Table 2 for the mixtures of cellulose cryogel particles and sunflower oil were in the range of  $G'$  ( $1\text{--}50 \times 10^5$  Pa) and yield stress (150–1000 Pa) values of most commercial fats (Calligaris et al., 2021; Patel, Nikolson et al., 2020). The rheological moduli values were not affected by temperature in the considered range (20–90 °C). Supplementary Fig. 1 shows that  $G'$  values remained constant upon temperature increase, indicating the absence of temperature-sensitive structures. Differently from food fats, based on crystal networks melting with temperature increase, the developed mixtures are based on cellulose, which is non-sensitive at temperatures within the studied range. Accordingly, no oil release was observed upon heating, which is important for food applications.

Although data from amplitude and frequency sweep tests suggest a rheological behaviour of the developed mixtures similar to that of commercial fats, the low deformations applied during these tests only partially describe the deformation behaviour of the developed materials. Thus, to further investigate the structure of cryogel-oil mixtures in the 71–74% oil range, spreadability tests were conducted, since this is a pivotal property of food fats. Fig. 3 reports the stress-strain curves of

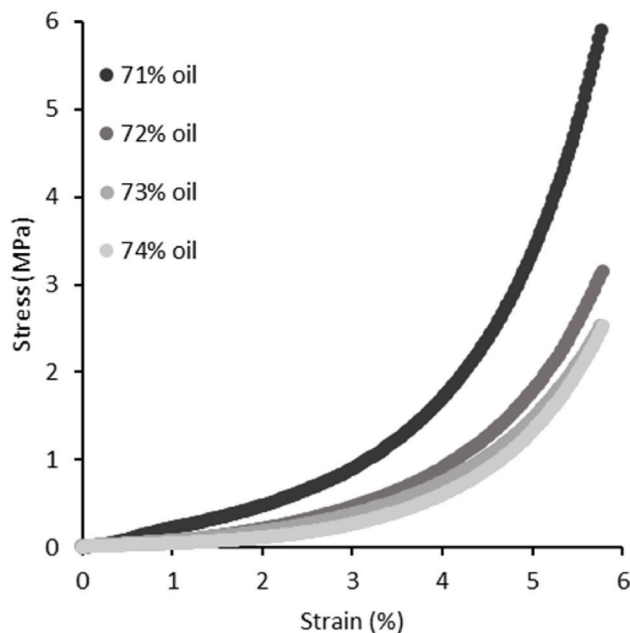


Fig. 3. Stress-strain curves of systems containing cellulose cryogel particles and increasing concentrations of sunflower oil from 71 to 74% (w/w).

these systems registered under compression. As expected, the increase in oil content promoted a shift of the curves towards lower values. Nevertheless, in all cases, an exponential increase ( $R^2 > 0.99$ ) of stress with the compressive displacement was observed. This behavior indicates that the obtained samples were not spreadable, being unable to distribute themselves around the compressive head during its downstream movement. Rather, the samples tended to compact under the tool, accounting for the observed force increase.

Systems containing cellulose cryogel particles and sunflower oil in the 71–74 % (w/w) range were also stored at ambient conditions for up to 4 months. Assessment of OHC (data not shown) demonstrated that no oil release was observed during this period.

Overall, the collected data indicate that cryogel particles effectively structure the oil forming a semi-solid material with high physical stability and rheological properties similar to those of food fats but not presenting a plastic behavior. The latter is linked to the presence of a fat crystal network in food products, providing the typical fat spreadability (Rogers, Tang, Ahmadi, & Marangoni, 2008). It can be hypothesized that cellulose cryogel particles mainly absorbed the oil into the cryogel pores and formed capillary bridges between adjacent particles. Nevertheless, the particles were not able to engage in the formation of a continuous plastic network. Based on these considerations, the resulting materials could be regarded as granular solids. It can be hypothesized that the decrease of the size and the modulation of the shape of the developed cryogel particles can be exploited to further tune their oil structuring capacity as well as the rheological and spread behaviour (Bonn, Denn, Berthier, Divoux, & Manneville, 2017; Fuhrmann, Powell, & Rousseau, 2023; Møller & Bonn, 2007; Nishinari et al., 2024). Moreover, begetting spheroidal-shaped particles of dimension lower than 25–50  $\mu\text{m}$  would be particularly convenient for food applications, since these particle morphological features would avoid sensory graininess perception.

### 3.3. Cellulose oleogels under gastrointestinal conditions

Due to the possible effect of the oil structuring on the digestion behavior (Alongi et al., 2022; Ciuffarin, Alongi, et al., 2023; Plazzotta et al., 2022), the suspension oleogel containing cellulose cryogel particles and 71% (w/w) sunflower oil was submitted to *in vitro* simulated digestion, and compared to a control sample, containing MCC and

sunflower oil at the same oil concentration. The destructuring behavior of the oleogel containing cellulose cryogel particles upon the gastric and intestinal phases was first observed by confocal microscopy (Fig. 4).

As seen in Fig. 4A, at the end of the gastric phase of the system cryogel particles-oil, a limited number of round oil droplets (yellow) was observed, probably due to the swelling of cellulose particles (turquoise) upon contact with the aqueous digestive environment. Cellulose cryogels have been indeed shown to undergo intense water absorption (Ciuffarin, Négrier, et al., 2023), which probably accounted for the formation of a swollen system embedding and masking the oil during the confocal microscopy analysis. Conversely, as shown in Fig. 4B, oil droplets were evident at the end of the intestinal phase, along with cellulose fragments. It can be hypothesized that the dilution of the digestive system due to the addition of intestinal fluids induced further swelling of cellulose cryogel particles and, consequently, oil release and droplet coalescence. The suggestion of cellulose cryogel particles swelling in water at pH 7–8 is supported by cellulose surface hydrophilicity due to a high density of hydroxyl groups (Yamane et al., 2006), provided cellulose is dissolved in aqueous NaOH and coagulated in water which is the case of our cryogel preparation. Similar confocal micrographs at the intestinal level were observed upon the digestion of unstructured oil in our previous works (Ciuffarin, Alongi, et al., 2023; Plazzotta et al., 2022). This comparison suggests that cellulose cryogel particles did not interfere with intestinal oil digestion, probably due to their strong hydrophilic nature, associated with digestion resistance. To confirm this hypothesis, the analysis of FFA released during intestinal digestion was conducted (Fig. 5).

The release of free fatty acids (FFA) during intestinal digestion exhibited a pattern consistent with prior studies (Ciuffarin, Alongi, et al., 2023; Li et al., 2011; O'Sullivan et al., 2017), with a rapid increase in the initial phase, followed by a gradual slowing down of FFA release until reaching a *plateau*. After 2 h of intestinal digestion, both cellulose oleogel and the control containing MCC and oil showed a comparable FFA release of around 52%. This value is in line with the hydrolysis level of unstructured sunflower oil (Calligaris et al., 2020). Moreover, no differences between the digested cellulose oleogel and the control were found in terms of oil particle size distribution (Fig. 6) and zeta potential (around  $-67$  mV in both cases).

These findings showed that the structuring of oil into a cellulose oleogel did not affect the digestion behavior of oil. This is probably due to the tendency of cellulose to release oil in the early stages of gastrointestinal digestion, thus being unable to protect it from the action of lipolytic enzymes. By contrast, in our previous study relevant to the digestion of whey protein-based oleogels (Ciuffarin, Alongi, et al., 2023), it was found that protein particles favored oil digestion at the intestinal phase. As a consequence, the use of cellulose oleogels in foods as fat replacers would not affect the nutritional functionalities of the structured oil.

## 4. Conclusions

This study demonstrates the feasibility of using cellulose cryogel particles to structure liquid oil. Materials presenting rheological moduli and yield stress similar to those of traditional food fats and high physical stability can be obtained in a specific oil content range (71–74%, w/w). These systems do not present the plastic deformation behavior typical of fat crystal networks. The capability of cellulose particles to entrap oil was attributed to their ability to absorb oil and to the formation of oil capillary bridges among the particles, leading to systems that can be regarded as granular solids. Interestingly, oil structuring by cellulose particles was not affected by temperature and also did not affect the rate and extent of lipolysis upon *in vitro* digestion.

The obtained results open the prospects of exploiting powders made of freeze-dried ground cellulose hydrogels as oleogelators in the food sector. In particular, rather than alternatives to traditional fats with plastic rheological behavior, cellulose cryogel particles are promising

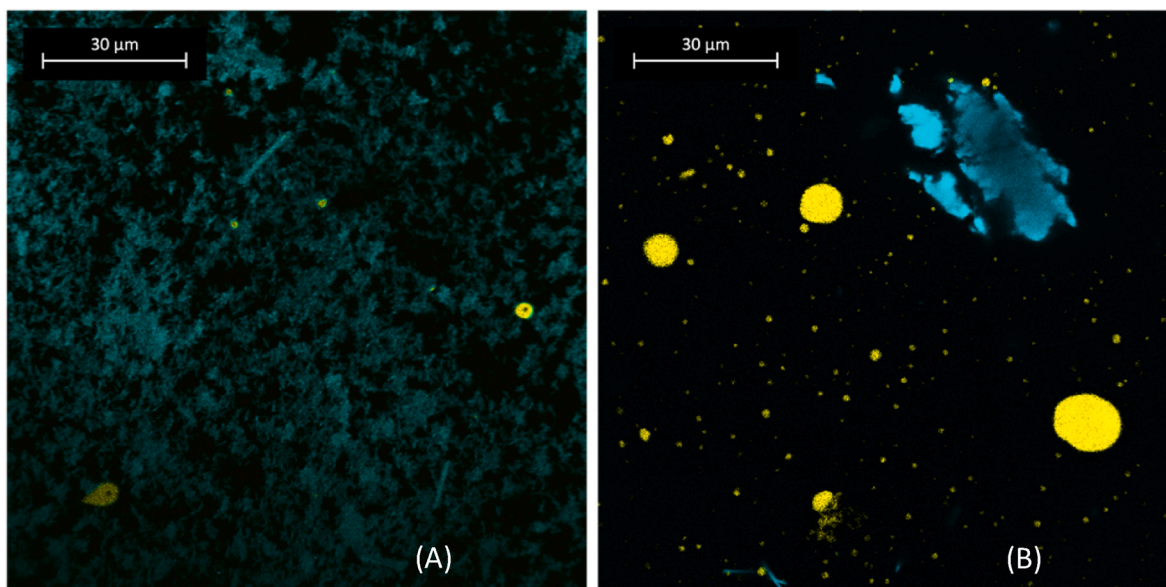


Fig. 4. Confocal micrographs of the gastric (A) and intestinal (B) digestate samples of an oleogel containing cellulose cryogel particles and 71% (w/w) sunflower oil. Cellulose is represented in turquoise, and oil in yellow.

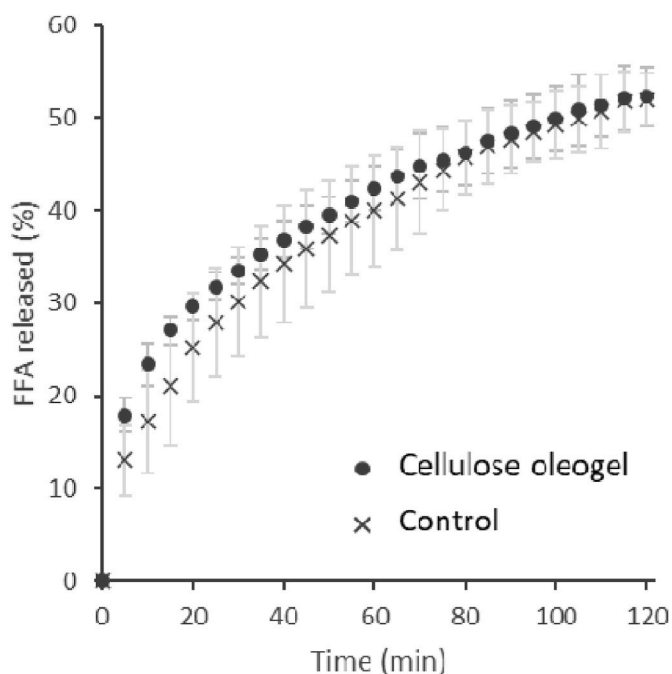


Fig. 5. Free fatty acid (FFA) release kinetics during *in vitro* intestinal digestion of an oleogel containing cellulose cryogel particles and 71% (w/w) sunflower oil (“cellulose oleogel”). The sample containing MCC and 71% (w/w) sunflower oil is shown as “control”.

ingredients to hinder oil separation or favor homogeneous oil distribution.

**CRedit authorship contribution statement**

**Francesco Ciuffarin:** Writing – original draft, Visualization, Methodology, Investigation, Formal analysis, Data curation. **Stella Plaz-zotta:** Writing – review & editing, Visualization, Methodology, Investigation, Data curation, Conceptualization. **Loris Gelas:** Writing – review & editing, Methodology, Investigation. **Sonia Calligaris:** Writing

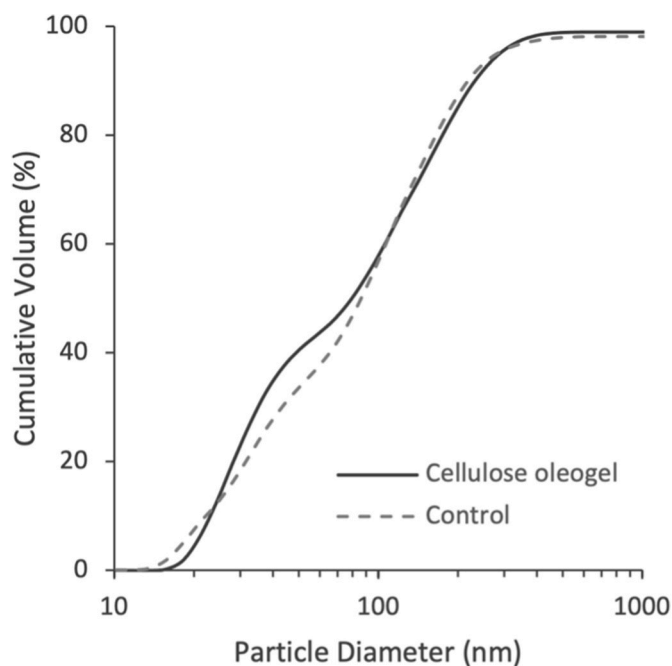


Fig. 6. Cumulative particle size distribution after *in vitro* intestinal digestion of an oleogel containing cellulose cryogel particles and 71% (w/w) sunflower oil (“cellulose oleogel”). The sample containing MCC and 71% (w/w) sunflower oil is shown as “control”.

– review & editing, Methodology, Conceptualization. **Tatiana Budtova:** Writing – review & editing, Supervision, Funding acquisition, Conceptualization. **Lara Manzocco:** Writing – review & editing, Supervision, Funding acquisition, Conceptualization.

**Declaration of competing interest**

The authors declare that they have no known competing financial interests or personal relationships that could have appeared to influence the work reported in this paper.

## Data availability

Data will be made available on request.

## Acknowledgements

Work was carried out in the framework of COST Action CA18125 “Advanced Engineering and Research of aeroGels for Environment and Life Sciences” (AEROGELS), funded by the European Commission.

## Appendix A. Supplementary data

Supplementary data to this article can be found online at <https://doi.org/10.1016/j.foodhyd.2024.110470>.

## References

- Alavi, F., & Ciftci, O. N. (2023). Superlight macroporous aerogels produced from cold-set egg white protein hydrogels show superior oil structuring capacity. *Food Hydrocolloids*, 136, Article 108180. <https://doi.org/10.1016/j.foodhyd.2022.108180>
- Ashkar, A., Laufer, S., Rosen-Kligvasser, J., Lesmes, U., & Davidovich-Pinhas, M. (2019). Impact of different oil gelators and oleogelation mechanisms on digestive lipolysis of canola oil oleogels. *Food Hydrocolloids*, 97, Article 105218. <https://doi.org/10.1016/j.foodhyd.2019.105218>
- Blake, A. I., & Marangoni, A. G. (2015). The effect of shear on the microstructure and oil binding capacity of wax crystal networks. *Food Biophysics*, 10, 403–415. <https://doi.org/10.1007/s11483-015-9398-z>
- Bonn, D., Denn, M. M., Berthier, L., Divoux, T., & Manneville, S. (2017). Yield stress materials in soft condensed matter. *Reviews of Modern Physics*, 89, Article 035005. <https://doi.org/10.1103/RevModPhys.89.035005>
- Brodkorb, A., Egger, L., Alminger, M., Alvito, P., Assunção, R., Ballance, S., et al. (2019). INFOGEST static in vitro simulation of gastrointestinal food digestion. *Nature Protocols*, 14, 991–1014. <https://doi.org/10.1038/s41596-018-0119-1>
- Brunauer, S., Emmett, P. H., & Teller, E. (1938). Adsorption of gases in multimolecular layers. *Journal of the American Chemical Society*, 60, 309–319. <https://doi.org/10.1021/ja01269a023>
- Calligaris, S., Alongi, M., Lucci, P., & Anese, M. (2020). Effect of different oleogelators on lipolysis and curcuminoid bioaccessibility upon in vitro digestion of sunflower oil oleogels. *Food Chemistry*, 314, 126–146. <https://doi.org/10.1016/j.foodchem.2019.126146>
- Calligaris, S., Plazzotta, S., Barba, L., & Manzocco, L. (2021). Design of roll-in margarine analogous by partial drying of monoglyceride-structured emulsions. *European Journal of Lipid Science and Technology*, 123, Article 2000206. <https://doi.org/10.1002/ejlt.202000206>
- Ciuffarin, F., Alongi, M., Plazzotta, S., Lucci, P., Schena, F. P., Manzocco, L., et al. (2023). Oleogelation of extra virgin olive oil by different gelators affects lipid digestion and polyphenol bioaccessibility. *Food Research International*, 173, Article 113239. <https://doi.org/10.1016/j.foodres.2023.113239>
- Ciuffarin, F., Négrier, M., Plazzotta, S., Libralato, M., Calligaris, S., Budtova, T., et al. (2023). Interactions of cellulose cryogels and aerogels with water and oil: Structure-function relationships. *Food Hydrocolloids*, 140, Article 108631. <https://doi.org/10.1016/j.foodhyd.2023.108631>
- De Vries, A., Gomez, Y. L., Van der Linden, E., & Scholten, E. (2017). The effect of oil type on network formation by protein aggregates into oleogels. *RSC Advances*, 7, 11803–11812. <https://doi.org/10.1039/c7ra00396j>
- De Vries, A., Lopez Gomez, Y., Jansen, B., Van der Linden, E., & Scholten, E. (2017). Controlling agglomeration of protein aggregates for structure formation in liquid oil: A sticky business. *ACS Applied Materials and Interfaces*, 9, 10136–10147. <https://doi.org/10.1021/acsami.7b00443>
- Dent, T., Hallinan, R., Chitchumroonchokchai, C., & Maleky, F. (2022). Rice bran wax structured oleogels and in vitro bioaccessibility of curcumin. *Journal of the American Oil Chemists' Society*, 99, 299–311. <https://doi.org/10.1002/aocs.12576>
- Druel, L., Niemeyer, P., Milow, B., & Budtova, T. (2018). Rheology of cellulose-[DBNH][CO<sub>2</sub>Et] solutions and shaping into aerogel beads. *Green Chemistry*, 20, 3993–4002. <https://doi.org/10.1039/c8gc01189c>
- Fuhrmann, P. L., Powell, J., & Rousseau, D. (2023). Structure and rheology of oil-continuous capillary suspensions containing water-swelling cellulose beads and fibres. *Food Hydrocolloids*, 139, Article 108503. <https://doi.org/10.1016/j.foodhyd.2023.108503>
- Gallier, S., Gordon, K. C., & Singh, H. (2012). Chemical and structural characterisation of almond oil bodies and bovine milk fat globules. *Food Chemistry*, 132, 1996–2006. <https://doi.org/10.1016/j.foodchem.2011.12.038>
- Hervik, A. K., & Svihus, B. (2019). The role of fiber in energy balance. *Journal of Nutrition and Metabolism*, 2019, Article 4983657. <https://doi.org/10.1155/2019/4983657>
- Hooper, L., Martin, N., Jimoh, O. F., Kirk, C., Foster, E., & Abdelhamid, A. S. (2020). Reduction in saturated fat intake for cardiovascular disease. *Cochrane Database of Systematic Reviews*, 19, Article CD011737. <https://doi.org/10.1002/14651858.CD011737.pub3>
- Jiang, Y., Liu, L., Wang, B., Sui, X., Zhong, Y., Zhang, L., et al. (2018). Cellulose-rich oleogels prepared with an emulsion-templated approach. *Food Hydrocolloids*, 77, 460–464. <https://doi.org/10.1016/j.foodhyd.2017.10.023>
- Jung, I., Schroeter, B., Plazzotta, S., De Berardinis, L., Smirnova, I., Gurikov, P., et al. (2023). Oleogels from mesoporous whey and potato protein based aerogel microparticles: Influence of microstructural properties on oleogelation ability. *Food Hydrocolloids*, 142, Article 108758. <https://doi.org/10.1016/j.foodhyd.2023.108758>
- Li, Y., Hu, M., Du, Y., Xiao, H., & McClements, D. J. (2011). Control of lipase digestibility of emulsified lipids by encapsulation within calcium alginate beads. *Food Hydrocolloids*, 25, 122–130. <https://doi.org/10.1016/j.foodhyd.2010.06.003>
- Luo, N., Ye, A., Wolber, F. M., & Singh, H. (2021). Effect of gel structure on the in vitro gastrointestinal digestion behaviour of whey protein emulsion gels and the bioaccessibility of capsaicinoids. *Molecules*, 26, Article 26051379. <https://doi.org/10.3390/molecules26051379>
- Mahdi, F., Hassanpour, A., & Muller, F. (2018). An investigation on the evolution of granule formation by in-process sampling of a high shear granulator. *Chemical Engineering Research and Design*, 129, 403–411. <https://doi.org/10.1016/j.cherd.2017.10.038>
- Manzocco, L., Mikkonen, K. S., & García-González, C. A. (2021). Aerogels as porous structures for food applications: Smart ingredients and novel packaging materials. *Food Structure*, 28, Article 100188. <https://doi.org/10.1016/j.foostr.2021.100188>
- Marangoni, A. G., & Garti, N. (2018). *Edible oleogels: Structure and health implications* (2 ed.). Elsevier. <https://doi.org/10.1016/C2015-0-02413-3>
- Marangoni, A. G., Idziak, S. H. J., Vega, C., Batte, H., Ollivon, M., Jantzi, P. S., et al. (2007). Encapsulation-structuring of edible oil attenuates acute elevation of blood lipids and insulin in humans. *Soft Matter*, 3, 183–187. <https://doi.org/10.1039/b611985a>
- Martins, A. J., Vicente, A. A., Cunha, R. L., & Cerqueira, M. A. (2018). Edible oleogels: An opportunity for fat replacement in foods. *Food & Function*, 9, 758–773. <https://doi.org/10.1039/c7fo01641g>
- Mat, D. J. L., Le Feunteun, S., Michon, C., & Souchon, I. (2016). In vitro digestion of foods using pH-stat and the INFOGEST protocol: Impact of matrix structure on digestion kinetics of macronutrients, proteins and lipids. *Food Research International*, 88, 226–233. <https://doi.org/10.1016/j.foodres.2015.12.002>
- Meng, Z., Qi, K., Guo, Y., Wang, Y., & Liu, Y. (2018). Effects of thickening agents on the formation and properties of edible oleogels based on hydroxypropyl methyl cellulose. *Food Chemistry*, 246, 137–149. <https://doi.org/10.1016/j.foodchem.2017.10.154>
- Møller, P. C., & Bonn, D. (2007). The shear modulus of wet granular matter. *Europhysics Letters*, 80, Article 38002. <https://doi.org/10.1209/0295-5075/80/38002>
- Mu, R., Hong, X., Ni, Y., Li, Y., Pang, J., Wang, Q., et al. (2019). Recent trends and applications of cellulose nanocrystals in food industry. *Trends in Food Science and Technology*, 93, 136–144. <https://doi.org/10.1016/j.tifs.2019.09.013>
- Nishinari, K., Ishihara, S., Nakauma, M., Funami, T., Zhu, C., Zhang, K., ... Singh, N. (2024). Rheology of bolus as a wet granular matter—Influence of saliva on rheology of polysaccharide gel beads. *Food Hydrocolloids*, 150, Article 109704. <https://doi.org/10.1016/j.foodhyd.2023.109704>
- O'Sullivan, C. M., Davidovich-Pinhas, M., Wright, A. J., Barbut, S., & Marangoni, A. G. (2017). Ethylcellulose oleogels for lipophilic bioactive delivery—effect of oleogelation on: In vitro bioaccessibility and stability of beta-carotene. *Food & Function*, 8, 1438–1451. <https://doi.org/10.1039/c6fo01805j>
- Papoutsis, K., Golding, J. B., Vuong, Q., Pristijono, P., Stathopoulos, C. E., Scarlett, C. J., et al. (2018). Encapsulation of citrus by-product extracts through spray-drying and freeze-drying using combinations of maltodextrin with soybean protein and L-carrageenan. *Foods*, 7, Article 7070115. <https://doi.org/10.3390/foods7070115>
- Patel, A. R. (2020). Biopolymer-based oleocolloids. In K. Pal, I. Banerjee, P. Sarkar, D. Kim, W. P. Deng, N. K. Dubey, et al. (Eds.), *Biopolymer-based formulations: Biomedical and food applications* (pp. 587–604). Elsevier. <https://doi.org/10.1016/B978-0-12-816897-4.00024-2>
- Patel, A. R., Nicholson, R. A., & Marangoni, A. G. (2020). Applications of fat mimetics for the replacement of saturated and hydrogenated fat in food products. *Current Opinion in Food Science*, 33, 61–68. <https://doi.org/10.1016/j.cofs.2019.12.008>
- Plakantonaki, S., Roussis, I., Bilalis, D., & Priniotakis, G. (2023). Dietary fiber from plant-based food wastes: A comprehensive approach to cereal, fruit, and vegetable waste valorization. *Processes*, 11, Article 11051580. <https://doi.org/10.3390/PR11051580>
- Plazzotta, S., Alongi, M., De Berardinis, L., Melchior, S., Calligaris, S., & Manzocco, L. (2022). Steering protein and lipid digestibility by oleogelation with protein aerogels. *Food & Function*, 13, 10601–10609. <https://doi.org/10.1039/d2fo01257j>
- Plazzotta, S., Calligaris, S., & Manzocco, L. (2020). Structural characterization of oleogels from whey protein aerogel particles. *Food Research International*, 132, Article 109099. <https://doi.org/10.1016/j.foodres.2020.109099>
- Plazzotta, S., Jung, I., Schroeter, B., Subrahmanyam, R. P., Smirnova, I., Calligaris, S., et al. (2021). Conversion of whey protein aerogel particles into oleogels: Effect of oil type on structural features. *Polymers*, 13, 4063. <https://doi.org/10.3390/polym13234063>
- Rogers, M. A., Tang, D., Ahmadi, L., & Marangoni, A. G. (2008). Fat crystal networks. In J. M. Aguilera, & P. J. Lillford (Eds.), *Food materials science*. New York, NY: Springer. <https://doi.org/10.1007/978-0-387-71947-4.17>
- Sabet, S., Pinto, T. C., Kirjoranta, S. J., Garcia, A. K., & Valoppi, F. (2023). Clustering of oleogel production methods reveals pitfalls and advantages for sustainable, upscalable, and oxidative stable oleogels. *Journal of Food Engineering*, 357, Article 111659. <https://doi.org/10.1016/j.jfoodeng.2023.111659>
- Salvia-Trujillo, L., Verkempinck, S. H. E., Sun, L., Van Loey, A. M., Grauwet, T., & Hendrickx, M. E. (2017). Lipid digestion, micelle formation and carotenoid



- bioaccessibility kinetics: Influence of emulsion droplet size. *Food Chemistry*, 229, 653–662. <https://doi.org/10.1016/j.foodchem.2017.02.146>
- Schatteman, D. (2013). *Alternative routes to oil structuring using oleogelators*. Springer. <https://lib.ugent.be/catalog/rug01:002063626>.
- Selmer, I., Karnetzke, J., Kleemann, C., Lehtonen, M., Mikkonen, K. S., Kulozik, U., et al. (2019). Encapsulation of fish oil in protein aerogel micro-particles. *Journal of Food Engineering*, 260, 1–11. <https://doi.org/10.1016/j.jfoodeng.2019.04.016>
- Silva, R. C. da, Ferdous, M. J., Foguel, A., & da Silva, T. L. T. (2023). Oleogels as a fat substitute in food: A current review. *Gels*, 9, 180. <https://doi.org/10.3390/gels9030180>
- Sun, C. (2005). True density of microcrystalline cellulose. *Journal of Pharmaceutical Sciences*, 94, 2132–2134. <https://doi.org/10.1002/jps.20459>
- Uddin, M. K., Mahmud, M. R., Hasan, S., Peltoniemi, O., & Oliviero, C. (2023). Dietary micro-fibrillated cellulose improves growth, reduces diarrhea, modulates gut microbiota, and increases butyrate production in post-weaning piglets. *Scientific Reports*, 13, 6194. <https://doi.org/10.1038/S41598-023-33291-Z>
- Vehovec, T., Gartner, A., Planinček, O., & Obreza, A. (2012). Influence of different types of commercially available microcrystalline cellulose on degradation of perindopril erbumine and enalapril maleate in binary mixtures. *Acta Pharmaceutica*, 62, 515–528. <https://doi.org/10.2478/v10007-012-0039-5>
- Yamane, C., Aoyagi, T., Ago, M., Sato, K., Okajima, K., & Takahashi, T. (2006). Two different surface properties of regenerated cellulose due to structural anisotropy. *Polymer Journal*, 38, 819–826.
- Younes, M., Aggett, P., Aguilar, F., Crebelli, R., Di Domenico, A., ... Woutersen, R. A. (2018). Re-evaluation of celluloses E 460 (i), E 460 (ii), E 461, E 462, E 463, E 464, E 465, E 466, E 468 and E 469 as food additives. *EFSA Journal*, 16, Article e05047.
- Zhao, W., Wei, Z., & Xue, C. (2022). Recent advances on food-grade oleogels: Fabrication, application and research trends. *Critical Reviews in Food Science and Nutrition*, 62, 7659–7676. <https://doi.org/10.1080/10408398.2021.1922354>